2021 43rd Annual International Conference of the
IEEE Engineering in Medicine & Biology Society (EMBC)
Oct 31 - Nov 4, 2021. Virtual Conference

Control of a Mechanical Blood Pump based on a Trade-off between Aortic Valve Dynamics and Cardiac Outputs*

Jeongeun Son, Dongping Du, and Yuncheng Du, *Member, IEEE*

***Abstract*—Left ventricular assist device (LVAD) is a therapeutic option for advanced heart failure (HF) patients. This mechanical device assists a failing heart to circulate blood in the human body by adjusting its pump speed according to cardiac output. However, to use an LVAD for *bridge-to-recovery*, other criteria (e.g., aortic valve function) should be also considered to reduce complications of the LVAD implantation. In this work, we present an optimization-based control approach to meet the circulatory demand of blood, while maintaining the aortic valve to open and close repeatedly in a cardiac cycle. To validate the performance of the control method, several case studies were investigated, which incorporate different levels of HF severity and physical activity. The results show that the optimization-based control algorithm can quantify the trade-off between the aortic valve function and the blood flow, which will meet clinicians' long quest to improve the myocardial functions for the use of an LVAD as *bridge-to-recovery*.**

***Clinical Relevance*—The efficacy of the control algorithm was validated with computer experiments, showing its potential as a bridge to recovery or as a long-term treatment plan for HF.**

I. INTRODUCTION

Heart disease is well-known as one of the leading causes of mortality worldwide. It is estimated that about 6.5 million patients in the U.S. undergo heart failure (HF) [1], which is a disease condition that the heart is unable to pump sufficient blood out of the left ventricle as it should. Although heart transplantation is identified as the best therapeutic option for advanced HF, not all patients can receive heart transplantation surgery because of the lack of available organ donors. As a treatment option, a rotary left ventricular assist device (LVAD) can be surgically implanted to provide a temporary mechanical support for a failing heart until donor organs become available, which is termed *bridge-to-transplantation*. Recently, it has been reported that myocardial functions can be improved with the support of the LVAD [2]. Thus, there has been a growing interest to use LVADs for *bridge-to-recovery* to assist patients to restore the impaired myocardial function. The reverse of HF will be able to allow the implanted LVADs to be removed from the patients so that the patients can return to their normal lives.

A main challenge to use an LVAD for *bridge-to-recovery* is to maintain periodic opening and closing of the aortic valve in each cardiac period [3]. The switch in a precise sequence is essential to the recovery of myocardial functions. The aortic valve opens only when the aortic pressure becomes lower than the left ventricular pressure. When an LVAD is implanted, the pressure in the left ventricle is affected by the constant unloading through the LVAD. For example, the left ventricular pressure will be lower than the aortic pressure if the pump is operated at high speed. In this case, the aortic valve will be permanently shut down. When it happens, the LVAD only pumps the blood in the left ventricle out, and the aortic valve is bypassed. Such a permanent closure of the aortic valve poses a deleterious threat to the myocardial recovery of the heart [4].

To assure that the pump does not replace the heart's pumping function and maximize the cardiac output, it is essential to incorporate the aortic valve dynamics when the pump speed is regulated [3], [5]. To address this, an optimization problem is presented in this work to find a trade-off between these two objectives. The control design can find the optimal solution using the concept of penalty weights on controlled outputs, i.e., cardiac output and aortic valve functions. In addition, since the aortic valve dynamics depend on different physiological conditions such as the intensity of physical activity and HF severity, the performance of the control algorithm is demonstrated with several case studies for two different levels of physical activity and HF severity.

This paper has three subsections. Section II provides the nonlinear dynamic model of the cardiovascular system coupled with an LVAD and formulates an optimization problem to tune the speed of an LVAD pump. The results of computer simulations are presented in Section III, and Section IV summarizes the conclusion of this work.

II. BACKGROUND AND METHODOLOGY

A. Model of the Cardiovascular-LVAD System

Several dynamic models to describe the cardiovascular system with an LVAD have been reported [3], [6], which have different levels of complexity. In this work, we use a lumped model in our previous work [6] for the cardiovascular system managed by an LVAD that has thirteen-dimensional nonlinear variables as follows:

$$\frac{dx}{dt} = \boldsymbol{P}(t)\boldsymbol{x} + \boldsymbol{Q}(t)s(\boldsymbol{x}) + ru(t) \tag{1}$$

where $\boldsymbol{x}$ denotes a vector of thirteen state variables listed in Table I, $\boldsymbol{P}(t)$ and $\boldsymbol{Q}(t)$ are (13×13) and (13×4) time-varying matrices, and $s(\boldsymbol{x})$ is a (4 × 1) vector that models the nonlinear behavior of the heart valves. Besides, r represents a (13 × 1) constant matrix. Note that $u(t) = \omega^2$ is the controlled

* This work is supported by National Science Foundation (CMMI-1646664, CMMI-1728338, and CMMI-1727487).

J. Son and Y. Du are with the Department of Chemical & Biomolecular Engineering, Clarkson University, Potsdam, NY 13699 USA (email: ydu@clarkson.edu).

D. Du is with the Department of Industrial, Manufacturing, & Systems Engineering, Texas Tech University, Lubbock, TX 43061 USA (e-mail: dongping.du@ttu.edu).

variable of the LVAD, where ω is the pump speed that will be optimized in this work. Details about the presented model and its parameters are given in [6].

TABLE I. SUMMARY OF VARIABLES IN THE HEART-LVAD MODEL [6].

Variable	Physiological Description	Unit
$x_1(t)$, $AoP(t)$	Aortic pressure	*mmHg*
$x_2(t)$, $Q_{AS}(t)$	Arterial systemic circulation blood flow	*ml/s*
$x_3(t)$, $ASP(t)$	Arterial systemic pressure	*mmHg*
$x_4(t)$, $Q_{VS}(t)$	Venous systemic circulation blood flow	*ml/s*
$x_5(t)$, $RAP(t)$	Right venous-atrial pressure	*mmHg*
$x_6(t)$, $RVP(t)$	Right ventricular pressure	*mmHg*
$x_7(t)$, $PAP(t)$	Pulmonary artery pressure	*mmHg*
$x_8(t)$, $Q_{AP}(t)$	Arterial pulmonary circulation blood flow	*ml/s*
$x_9(t)$, $APP(t)$	Arterial pulmonary pressure	*mmHg*
$x_{10}(t)$, $Q_{VP}(t)$	Venous pulmonary circulation blood flow	*ml/s*
$x_{11}(t)$, $LAP(t)$	Left venous-atrial pressure	*mmHg*
$x_{12}(t)$, $LVP(t)$	Left ventricular pressure	*mmHg*
$x_{13}(t)$, $Q_P(t)$	LVAD Pump flow	*ml/s*

To simulate the cardiovascular system with different physiological states, three hemodynamic parameters are considered in this work, which include the systemic vascular resistance (R_{sv}), pulmonary vascular resistance (R_{pv}), and maximum elastance of the left ventricle ($E_{max,lv}$). Note that the resistances R_{sv} and R_{pv} are used to define the levels of physical activity as described in [6], [7]. For instance, when the patients are active, smaller values of R_{sv} and R_{pv} are used. On the contrary, as the patients become less active, the values of both parameters increase. Besides, the maximum elastance $E_{max,lv}$ represents the contractility of the left ventricle. Thus, it is used to define the severity levels of HF.

It should be noted that some of these parameters can change over time due to the baroreflex system associated with short-term autonomic nerve regulation. Specifically, it maintains the hemodynamic system stable by regulating neural effectors [8], [9]. For accurate and reliable predictions, it is necessary to integrate the cardiovascular-LVAD system with the baroreflex system. Thus, in this work the baroreflex model proposed in Ursino [8] and Liu [9] was used, which consists of the afferent neural pathway, the efferent neural pathways, and a few distinct effectors. In this model, the afferent neural pathway is defined as the relationship between the activity of afferent nerves and arterial pressure. The efferent neural pathways are modeled by considering the frequency of spikes in the afferent fibers and its effects on the sympathetic fibers and vagal activity. Those stimulation activities result in the dynamic response of the effectors [8], [9]. In this work, four different effectors, i.e., systemic vascular resistance (R_{sv}), maximum elastance of ventricles ($E_{max,lv}$ and $E_{max,rv}$), and heart period (T_0), are controlled by the baroreflex model, which can be described as:

$$\alpha(t) = \alpha_0 + \Delta\alpha(t) \tag{2}$$

where α is the generic parameter representing the effectors over time, and $\Delta\alpha$ is the variation caused by the baroreflex regulation. Also, α_0 indicates each parameter in the absence of vagal and sympathetic activities. Details about the baroreflex model can be found in [8], [9].

To verify the accuracy of the model that consists of the heart, LVAD, and nerve regulation, several hemodynamic variables under the LVAD support were simulated, where the pump speed was set to 9000 rpm, and the simulation time was set to 55 seconds. Fig. 1 shows the results of consecutive cardiac cycles from 50 to 52 seconds for clarity. As seen, all hemodynamic waveforms show stable periodic predictions under the baroreflex system with the LVAD support. Note that the parameter values in the absence of cardiac innervation α_0 in (2), i.e., $R_{sv,0}$, $E_{max,lv0}$, $E_{max,rv0}$, and T_0, were set to 0.71 mmHg·s/mL, 1.0 mmHg/ml, 0.6 mmHg/ml, and 0.52 s, respectively [9]. By simulating the model, the controlled parameters α in (2), reached the stable values at the given pump speed of the LVAD (see Table II).

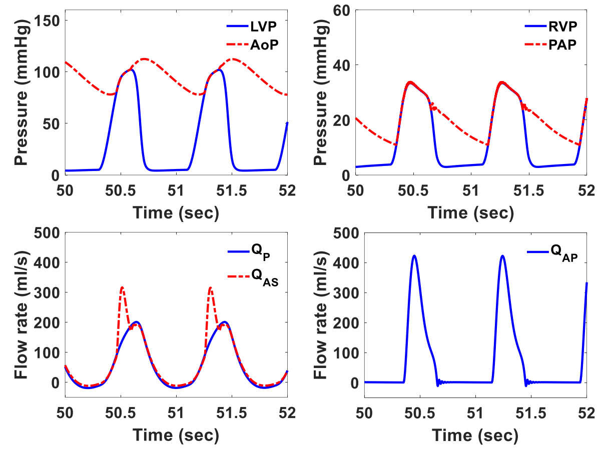

Figure 1. Simulated results for the hemodynamic waveforms with the LVAD support: (a) left ventricular pressure (LVP) and aortic pressure (AoP), (b) right ventricular pressure (RVP) and pulmonary arterial pressure (PAP), (c) pump flow (Q_P) and aortic flow (Q_{AS}), and (d) pulmonary arterial flow (Q_{AP}).

To further verify the cardiovascular-LVAD model under baroreflex regulation, we simulated the model with different levels of pump support. For the information on the unloading of the ventricles, the pressure-volume (P-V) loops of the left ventricle and right ventricle are given in Fig. 2 (a) and (b), respectively.

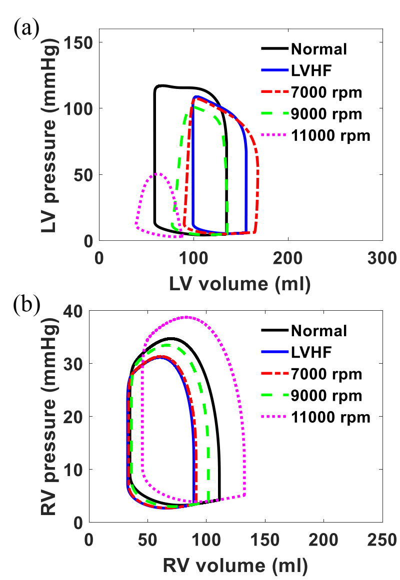

Figure 2. Simulated results for the P-V loops: (a) left ventricle and (b) right ventricle with different pump speeds of an LVAD (ω). LVHF stands for left ventricular heart failure.

As shown in Fig. 2 (a), as the pump speed increases, the P-V loop of the left ventricle is shifted to the left, and its area decreases due to reduced stroke work. In contrast to the P-V loop of the left ventricle, the right ventricular P-V loop is moved to the right, and its area increases, as illustrated in Fig. 2 (b).

The parameters R_{sv}, $E_{max,lv}$, $E_{max,rv}$, and T updated by the baroreflex control system are also summarized in Table II. When the pump speed was increased, it was also found that the resistance R_{sv} and the maximum elastance of ventricles $E_{max,lv}$ and $E_{max,rv}$ decrease, while the cardiac period T increased, as previously reported in [9]. This clearly shows the validity of the cardiovascular model managed by the LVAD under the baroreflex regulation.

TABLE II. SIMULATED EFFECTORS CONTROLLED BY BAROREFLEX SYSTEM WITH THREE DIFFERENT PUMP SPEEDS.

Pump Speed (ω)	R_{sv}	$E_{max,lv}$	$E_{max,rv}$	T
7000 rpm	1.0709	1.1842	0.9008	0.7826
9000 rpm	1.0449	1.1711	0.8794	0.7930
11000 rpm	0.9249	1.1126	0.7840	0.8518

B. Formulation of an Optimization Problem for Control

To quantify a periodical switch between the opening and closing of the aortic valve, we measured the aortic valve opening duration (AoD, %), which is defined as the ratio between the aortic opening time in a cardiac period and the time to complete a cycle [3]. As an example, Fig. 3 shows AoD and the cardiac output (CO, L/min) for different values of the pump speed ω, where $E_{max,lv0}$ was set to 1.0 mmHg/ml to describe a mild HF. The rest of model parameters, i.e., $R_{sv,0}$, $E_{max,rv0}$, and T_0, were set to 0.71 mmHg·s/mL, 0.6 mmHg/ml, and 0.52 s, respectively.

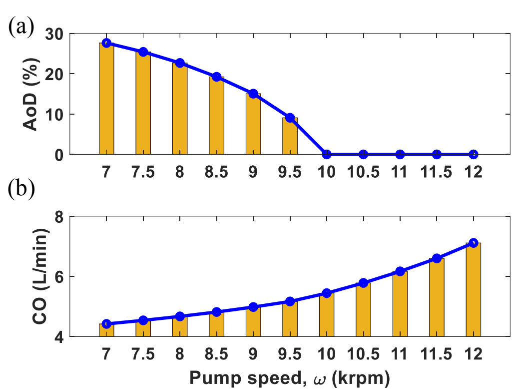

Figure 3. Simulated results for (a) aortic valve opening duration (AoD) and (b) cardiac output (CO) with different pump speeds (ω) of an LVAD.

As can be seen in Fig. 3 (b), CO increases constantly as the pump speed ω increases. In contrast, AoD decreases and eventually stabilizes at 0 as in Fig. 3 (a), when ω is increased. Note that the aortic valve is shut down permanently when AoD (%) is 0. As noted in Section I, the permanent closure of the aortic valve should be prevented to avoid detrimental effects on the myocardial recovery, when the use of the LVAD as *bridge-to-recovery* is considered.

To obtain the desired CO to support physiological activity and to maintain the aortic valve dynamics properly, an optimization problem is designed in this work, which can find a trade-off between these two objectives. The optimization is described as follows:

$$\min_{\lambda} J = w_1(CO - CO_{ref})^2 + w_2(AoD - AoD_{ref})^2 \qquad (3)$$

where w_1 and w_2 are two penalty weights that balance the cost of CO and AoD to the total cost in (3), and λ is the decision variable, i.e., ω, used to control the LVAD operation. It should be noted that the weights w_1 and w_2 are subject-specific and can be determined by clinicians to obtain the best recovery outcome for different patients with various myocardial conditions. In addition, CO_{ref} in (3) is a reference of desired CO that can be estimated with a model of a healthy heart [6]. Note that CO_{ref} should be selected considering the activity level of a patient. For example, a larger value can be used when the patient is active, e.g., mild exercise—walking stairs, since a larger amount of blood is required to satisfy the physiological demand needed for the patient's body. Further, AoD_{ref} is a reference of AoD determined by clinicians while considering the severity of HF, e.g., cardiac contractility. Specifically, as reported in [3], the maximum AoD for the HF patient is lower than the one with a hearty heart, and AoD decreases with the increase of the LVAD support level. Due to space issue, details about the appropriate selections of AoD_{ref} are not discussed. Table III shows the set-up of simulation parameters for four case scenarios studied in this work. Note that the ranges of HF severity and the intensity of physical activity in these case scenarios are chosen to ensure that the pump does not take over the pumping function of the heart completely. For the broader range of HF severity or intensity of physical activity, the aortic valve could be permanently closed, thus large changes in HF severity and intensity of activities are not considered here.

TABLE III. CASE CLASSIFICATION FOR SIMULATIONS

Case	$E_{max,lv0}$	$R_{sv,0}$	R_{pv}	CO_{ref}	AoD_{ref}	Physical meaning
1	0.75	0.71	0.14	5.182	27.43	Inactive
2	0.75	0.31	0.084	6.714	31.25	Moderately active
3	1.0	0.71	0.14	5.182	28.08	Inactive
4	1.0	0.31	0.084	6.714	31.85	Moderately active

* CO (L/min), AoD (%), $E_{max,lv0}$ (mmHg/ml), $R_{sv,0}$ and R_{pv} (mmHg/ml/s).

C. Constraints for Optimization Defined in (3)

Since the physiological states of HF patients can change over time, optimization of (3) should be executed in real-time. For safety concerns during the tuning of the pump speed of an LVAD, the following constraints are used in this work.

(i) *Constraints for CO*: For each optimization iteration in (3), the CO calculated with the decision variable λ should be above a minimum value, which ensures the blood demand of the human body. In this work, a constraint of CO in (3) is set to [4 L/min, 8 L/min].

(ii) *Constraints for AoD*: AoD is a function of the HF severity, activity level, and pump speed ω, and it is desired to maintain the aortic valve opening and closing in a precise sequence. A constraint [5 %, 32 %] is used for AoD in (3).

(iii) *Constraints for* ω: The controller of the LVAD should adjust ω properly to provide adequate blood while preventing overpumping and underpumping scenarios that can lead to ventricular suction and regurgitation, respectively. Therefore, a hard constraint of the pumping speed of an LVAD, [7 krpm, 12 krpm], is used for the decision variable λ in (3).

III. Results and Discussion

A. Summary of Optimization Results

The efficiency of the optimization-based control design of an LVAD is first studied for different cases as described in Table III, incorporating different levels of physical activity (R_{sv} and R_{pv}) and HF severity ($E_{max,lv}$). The first two cases (i.e., Cases 1 to 2) aim to compare the optimization results in terms of different intensities of physical activity of the patient implanted with an LVAD, while the last two cases (i.e., Cases 3 and 4) are used to study the effect of HF severity on the optimization results. The optimization results of (3) are briefly summarized in Table IV, for which the penalty weights are set to $w_1 = 1$ and $w_2 = 1\times10^{-3}$, respectively.

TABLE IV. Results of optimization (W_1=1, W_2=1E-03)

Results	Case 1	Case 2	Case 3	Case 4
ω (rpm)	8942.4	9085.1	8750.8	8750.8
CO (L/min)	4.672	6.2349	4.896	6.461
AoD (%)	12.906	13.380	17.230	18.534

As shown in Table IV, the optimization (3) can find the optimal solution to support the physiological demand of a HF patient in all case studies. For example, the decision variable ω in Case 1 was found to be ~8.94 krpm, and both *CO* and *AoD* were found to be within the ranges specified by the constraints as described in Section II. In addition, it was found that by comparing Case 1 to Case 2, *CO* increases as patients become more active, since a higher blood demand is required for an active patient. It was also found that the *AoD* is smaller for an inactive patient in Case 1. Note that only when the left ventricular pressure becomes higher than the aortic pressure, the aortic valve opens to allow blood to flow.

Additionally, as can be observed from case studies 1 to 4, the optimization results of (3) verify that it is necessary to take into account different levels of HF severity, while tuning the ω with respect to the physiological demand. For example, the native heart can provide necessary *CO* with less support from the LVAD for the reversed HF (see Cases 3 and 4), thus resulting in a higher *AoD* than the ones of Cases 1 and 2. Since the dynamic behavior of the aortic valve can be assured in a precise sequence in a cardiac period, the myocardial function recovery can be potentially improved.

B. Effect of Penalty Weights on Optimization

To assess the effect of the penalty weights in (3) on the control performance, a different set of weights was used in this case scenario. These two weights w_1 and w_2 were given as 1 and 2.5×10^{-3}, respectively. The simulation results with these penalty weights are briefly summarized in Table V.

TABLE V. Results of optimization (W_1=1, W_2=2.5E-03)

Results	Case 1	Case 2	Case 3	Case 4
ω (rpm)	8504.6	8544.2	8209.8	8313.1
CO (L/min)	4.528	6.004	4.729	6.2897
AoD (%)	17.376	18.849	21.299	21.9372

As seen in Table V, the penalty weights can affect the optimization results of (3). As compared to the results in Table IV, it was found that the *AoD* increases significantly, when w_2 is increased from 1×10^{-3} to 2.5×10^{-3}. For example, the *AoD* for Case 1 is increased from ~12.91 % to ~17.38 % (see Tables IV and V). As compared to the results of *AoD*, the *CO* decreases by ~3.08 % from ~4.67 L/min to ~4.53 L/min, for Case 1 with a different set of penalty weights in optimization (3).

In addition, it was found that the increment in *AoD* for the reversed HF is relatively smaller. For example, the *AoD* for Case 3 in Table V is ~21.30 % with a penalty weight $w_2 = 2.5\times10^{-3}$, which is only about ~4.07 % higher than the one obtained with a penalty weight $w_2 = 1\times10^{-3}$ in Table IV. A possible reason is that the *AoD*s in Cases 3 and 4 in Table IV are closer to the upper limits in the optimization constraints. Thus, the improvement in the *AoD* is relatively limited, as compared to other case studies such as Cases 1 and 2. Further, a considerable decrease in the optimization results of ω was observed in Table V, as compared to the results in Tables IV. This is because a larger penalty weight is used for *AoD*, which can greatly change the effect of *AoD* on the total cost in (3).

IV. Conclusion

An optimization-based control algorithm is developed in this work for the optimal tuning of the speed of an LVAD pump for *bridge-to-recovery*. Such optimization can find a proper balance to unload the left ventricle by the aortic valve and the LVAD. For the validation of the proposed control algorithm, four different case scenarios were studied, including different levels of physical activity (inactive and moderately active) and severity levels of heart failure (HF). The optimization results show that the optimized pump speed for each case scenario can ensure periodic opening and closing of the aortic valve in each cardiac period, while providing appropriate cardiac outputs. This will possibly improve the myocardial functions, when the LVAD is used for *bridge-to-recovery*. While only the aortic valve dynamics and cardiac output are considered in the optimization, additional criteria can be added when a clinician thinks it is necessary, which is not discussed for brevity.

References

[1] E. J. Benjamin et al., "Heart disease and stroke statistics—2018 update: a report from the American Heart Association," *Circulation*, vol. 137, no. 12, pp. e67–e492, Mar. 2018.

[2] D. Burkhoff, S. Klotz, and D. M. Mancini, "LVAD-induced reverse remodeling: basic and clinical implications for myocardial recovery," *J. Card. Fail.*, vol. 12, no. 3, pp. 227–239, Apr. 2006.

[3] G. Faragallah and M. A. Simaan, "An engineering analysis of the aortic valve dynamics in patients with rotary left ventricular assist devices," *J. Healthc. Eng.*, vol. 4, no. 3, pp. 307–327, May 2013.

[4] C. M. Carr, J. Jacob, S. J. Park, B. L. Karon, E. E. Williamson, and P. A. Araoz, "CT of left ventricular assist devices," *RadioGraphics*, vol. 30, no. 2, pp. 429–444, Mar. 2010.

[5] G. A. Wright et al., "A novel method of predicting aortic valve opening through LVAD power waveform analysis," *J. Heart Lung Transplant.*, vol. 32, no. 4, pp. S223, Apr. 2013.

[6] J. Son, D. Du, and Y. Du, "Modelling and control of a failing heart managed by a left ventricular assist device," *Biocybern. Biomed. Eng.*, vol. 40, no. 1, pp. 559–573, Jan.-Mar. 2020.

[7] Y. Wu, "Design and testing of a physiologic control system for an artificial heart pump," Ph.D. dissertation, Mech. Aerosp. Eng., Univ. Virginia, Charlottesville, VA, 2004.

[8] M. Ursino, "Interaction between carotid baroregulation and the pulsating heart: a mathematical model," *Am. J. Physiol. Heart Circ. Physiol.*, vol. 275, no. 5, pp. H1733–H1747, Nov. 1998.

[9] H. Liu, S. Liu, X. Ma, and Y. Zhang, "A numerical model applied to the simulation of cardiovascular hemodynamics and operating condition of continuous-flow left ventricular assist device," *Math. Biosci. Eng.*, vol. 17, no. 6, pp. 7519–7543, Oct. 2020.